ARTICLE

Atomic Force Microscopy Applied to Interrogate Nanoscale Cellular Chemistry and Supramolecular Bond Dynamics for Biomedical Applications

Received 00th January 20xx,
Accepted 00th January 20xx

DOI: 10.1039/x0xx00000x

Joshua D. Simpson,[a] Ankita Ray, [a] Melanie Koehler,[a] Danahe Mohammed[a] and David Alsteens*[a]

Understanding biological interactions at a molecular-level grants valuable information relevant to improving medical treatments and outcomes. Among the suite of technologies available, Atomic Force Microscopy (AFM) is unique in its ability to quantitatively probe forces and receptor-ligand interactions in real-time. The ability to assess the formation of supramolecular bonds and intermediates in real-time on surfaces and living cells generates important information relevant to understanding biological phenomena. Through combining AFM with fluorescence-based techniques allows for an unprecedented level of not only the formation and rupture of bonds, but understanding medically relevant interactions at a molecular level. As the ability of AFM to probe cells and more complex models improves, being able to assess binding kinetics, chemical topographies, and garner spectroscopic information will likely become key to developing further improvements in fields such as cancer, nanomaterials, and virology. The rapid response to the COVID-19 crisis, producing information regarding not just receptor affinities, but also strain-dependent efficacy of neutralizing nanobodies, demonstrates just how viable and integral to the pre-clinical development of information AFM techniques are in this era of medicine.

Introduction

Over the past decades, there has been a revolution in the manner in which Atomic Force Microscopy (AFM) can be applied to probe complex questions in biology. The evolution of AFM from a tool for assessing chemical and nanoscopic features of surfaces and materials towards an integral component of developing clinically-relevant information has been a steady progression, hastening in recent years. Being developed in 1986 initially as a tool to counter the topography of solid surfaces with atomic resolution,[1] AFM has rapidly risen through advances in the probes, sensors, computing power, and mechanisms for combining information with that produced by other techniques.[2,3] In this review, we briefly describe some of the current features and techniques in use for biological AFM applications, and highlight how the biomolecular understanding generated within this field is increasingly becoming relevant to the biomedical sector, particularly within the pre-clinical pipeline. Here we focus on the expanding biomedical relevance of AFM and applications specific for supporting preclinical research, rather than the broader review of AFM techniques and technologies reviewed elsewhere.[3] Further, we primarily highlight specific developments from our own research. Despite having arisen from humble beginnings, AFM is now poised to provide detailed information regarding complex biological processes, for example: the composition of the cell surface, underlying mechanics, and the binding and entry behaviours that mediate host-pathogen interactions. As the methodologies, equipment, data analyses, and chemistries of AFM have evolved, so too has the ability to provide insight into physiologically pertinent processes.

The basic principle of AFM is in comparison to many other techniques relatively simple: a nanoscopic tip attached to a cantilever is raster scanned close to the analysed sample. The interactions between the tip and the sample are probed through the deflection of the cantilever; measured by the reflection of a laser beam focused on the end of the cantilever into a photodiode. Using Hooke's law and the spring constant of the cantilever, the deflection can be translated into the force applied on the AFM tip (**Figure 1**). The surface topography is subsequently reconstructed with subnanometer precision via a feedback loop, which constantly re-adjusts the relative distance between sample and tip in order to keep their parameters of interaction constant. Depending on the AFM imaging mode, these parameters are: interaction force, oscillation amplitude, or frequency shift. Since the very early years of AFM development, the cantilever was also used as a force sensor to probe and extract a variety of physico-chemical and mechanical sample properties, such as chemical topography, stiffness, elasticity, and adhesion;[4] or in more advanced settings, specific interactions between biomolecules,[3] allowing for the determination of the kinetics of supramolecular bond formation. This mode, commonly known as force spectroscopy,

[a] *Louvain Institute of Biomolecular Science and Technology, Université Catholique de Louvain, Louvain-la-Neuve 1348, Belgium.*
Email : david.alsteens@uclouvain.be

† Footnotes relating to the title and/or authors should appear here.
Electronic Supplementary Information (ESI) available: [details of any supplementary information available should be included here]. See DOI: 10.1039/x0xx00000x

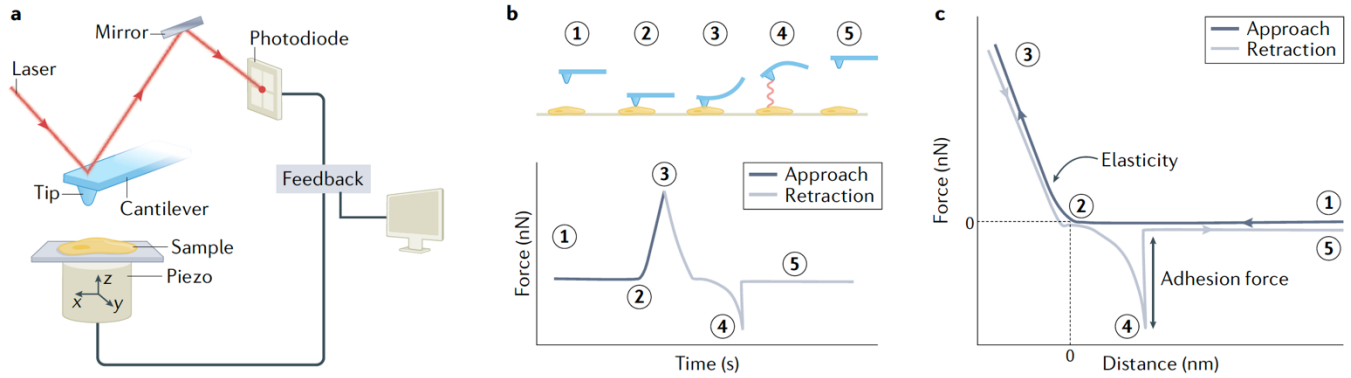

Figure 1: Basic principle of AFM. **(a)** as the cantilever raster scans the sample through movement of the piezo, deflection of the laser is detected using a photodiode, and feedback monitoring allows for continuous contact with the sample surface. **(b)** the approach **(1)** of the cantilever brings the tip into contact with the sample **(2)**, allowing for the establishment of a bond **(3)**, which during retraction is stretched **(4)**, until it ruptures **(5)**. An example of a FD curve showing an adhesion event as a plot of Force and time, wherein an FD curve corresponds to the event described **(c).** Reproduced from Viljoen *et al. Nat Rev Methods Primers*, 2021, **1**, 63, DOI: 10.1038/s43586-021-00062-x. Copyright © Viljoen *et al.* (DOI : 10.1038/s43586-021-00062-x).

is based on the acquisition of force-distance curves, wherein the stylus is cyclically approached and retracted from the surface while monitoring the variation of force with respect to the tip-sample distance. Forces ranging from the strength of individual receptor-ligand bonds (~tens picoNewtons [pN]) to those governing the adhesion of entire cells (>>1 nanoNewton (nN)) can be measured. By applying theoretical models, kinetic and thermodynamic parameters of receptor-ligand interactions can be extracted, leading to a complex picture of their binding free-energy landscape.[2,5] The ability to apply these techniques and understand the chemistry of complex biological interfaces has been facilitated through numerous advancements and achievements within the field, as highlighted below.

Milestones toward establishing AFM as a toolbox for cellular chemical imaging at the nanoscale

Already in the early 1990s, pioneering measurements of adhesion forces opened avenues for mapping the chemical properties of biological systems with chemically modified AFM tips and technical developments that have been constantly improving since then (**Figure 2**). After their invention, it was rapidly demonstrated that the functionalized cantilever allows for the detection of specific forces, while simultaneously being able to map the sample's topography and to extract its physico-chemical properties in a quantitative manner. This principle was first applied by the Lieber's group,[6] where they utilized an AFM tip functionalized with specific chemical groups to evidence hydrophilic and hydrophobic areas on pattered yet topographically smooth surfaces, paving the way for chemical force microscopy (CFM) and other mapping applications.[6] Shortly after, similar concepts and approaches were transferred to characterize biomolecular interactions such as the widely explored avidin-biotin[7–9] bond and other antibody-antigen systems,[10] by operating the AFM in single-molecule force spectroscopy mode with the tip upgraded to a biosensor (i.e., as chemical lab-on-the-tip). Together with the high spatial resolution, exceptional signal-to-noise ratio and the capability to be operated under nearly-physiological conditions, doors were opened to the sensing of specific biomolecular interactions, providing valuable insights into how molecular recognition contributes to the regulation of biological systems. Linking the underlying chemistry of interactions, *e.g.* covalent and supramolecular bond formation, to specific biological processes is of great importance. In this context, the functionalization of the AFM tip with single molecules is of crucial importance and several aspects needed to be considered for studying single molecule interactions in a specific manner. First, it was difficult to distinguish between specific and nonspecific interactions between the AFM tip and the biological sample, which usually originate from the direct contact between tip and sample. In addition, the direct grafting of biomolecules to the AFM tip could lead to steric effects, resulting in a decrease in binding probability. Furthermore, direct contact between biomolecules and the tip would reduce the molecule mobility and orientation, preventing specific interaction as well as leading to partial biomolecule denaturation. All of these factors are important to understanding the chemistry and kinetics of the interface between probe and sample.

A promising solution to tackle all these problems, was introduced by Hinterdorfer et al. first in 1996,[10] and further developed by the same group in 2011.[11] By functionalizing AFM tips with hydrophilic, flexible polyethylene glycol (PEG) linkers bearing functional end groups has enabled targeted, site-directed coupling of biomolecules through a variety of attachment strategies, and thus allow study of their specific recognition processes at the level of single interaction events. Swiftly, this procedure became, and remains, the gold standard for studying ligand-receptor interactions using SMFS and other advanced AFM applications. In terms of analysing single molecule interaction data, the characteristic nonlinear stretching of the linker before rupturing of the receptor-ligand bond provides a means to identify and analyse specific bond rupture events by classical polymer extension models, such as the worm-like chain (WLC) model.[12] Other early, pioneering applications include e.g. the direct measurement of forces between complementary strands of DNA[13] as well as

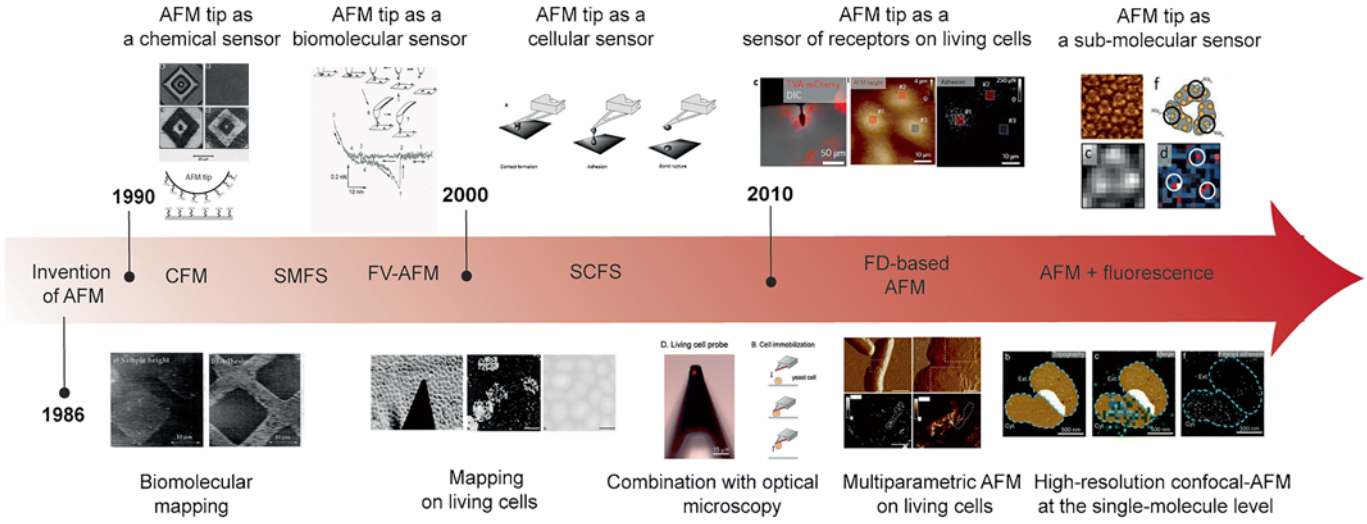

Figure 2: Timeline of important advances allowing for nanoscale analysis of biological samples. Important examples of tip modification and mapping strategies highlighted. Reproduced from Lo Giudice *et al*., *Anal Bioanal Chem*, 2019, **411,** 6549–6559.

mechanical investigations of protein structure through stretching and unfolding started to emerge.[14] Apart from using the AFM as a nanoscopic imaging or force spectroscopy tool, both modes can be combined to image biological systems at work, while simultaneously detecting, quantifying and topographically mapping biomolecular interactions. As pioneers in this field, Gaub's group demonstrated through "affinity imaging" the possibility to identify and localize specific biological interactions while simultaneously acquiring the topography and mechanical properties, first on a streptavidin patterned surface with a biotinylated tip,[7] and later on living red blood cells.[15,16] Immediately, force mapping emerged as an important tool and was consequently applied to a variety of bacterial[17] and mammalian cells, as well as for single-cell force spectroscopy applications (SCFS).[18] The latter is based on the immobilization of single living cells on a tipless AFM cantilever, allowing the measurement of novel biological parameters (e.g. direct cell-cell adhesion) at high spatial and force resolution, characteristic for AFM.[19] In parallel, the development of dynamic recognition modes started to come forth, enabling improvements regarding time and spatial resolution.[20–22]

In the last decade, AFM-based multiparametric imaging applied in molecular and cellular biology have witnessed a new revolution thanks to a variety of advanced technological developments.[23] Key breakthroughs include the development of environmental chambers to keep cells alive in physiological conditions for several days, paving the way for live mammalian cell AFM studies;[24] the development of faster and more sophisticated force-distance (FD) curve-based AFM methodologies[23]; and the coupling of AFM to optical microscopy techniques, ranging from epifluorescence to confocal (**Figure 3**) and super-resolution microscopes. Especially with the implementation of FD-based AFM, progress in terms of force control and data acquisition speed has allowed unprecedented progress in structurally mapping (bio)chemical interactions at molecular resolution.[3,23] The information provided by dual techniques providing complimentary information, that when combined provides unparalleled insight into the relationship between supramolecular bond formation and biological functionality.

In addition, a new generation of AFM tip manipulation strategies have emerged, for instance, Koehler et al. recently introduced photocleavable linkers to control the ligand-binding specificity in AFM force spectroscopy experiments and to deliver single molecules with high spatiotemporal resolution.[25] In another approach, the tip is modified by equipping the AFM with the recently established Fluidic Force Microscopy (Fluid-FM) technology.[26] With this innovative tool, the beads (or cells, colloids, other biomolecules) can be elegantly trapped (and released/injected) via a pressure controller upgrading the microchanneled cantilever to a force-controlled nanopipette or -syringe. Additionally, specific adhesion events can be localized at high resolution (~10 nm) on cellular surfaces.[3,23]

Given these improvements and rapidly expanding capabilities, it is not surprising to see that AFM has become increasingly used as part of pre-clinical studies. The information garnered being

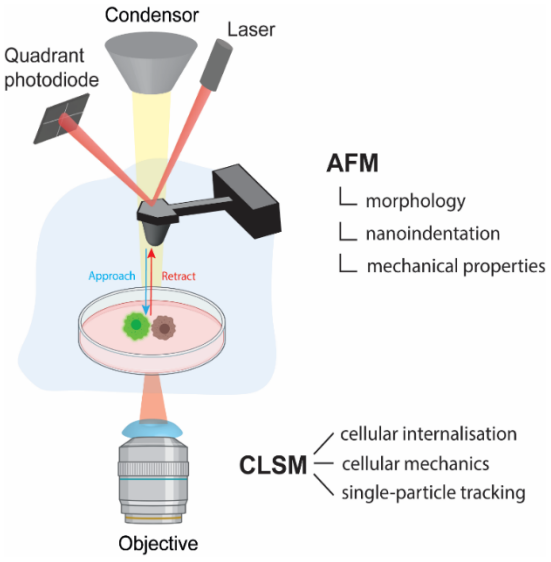

Figure 3: Combined confocal-AFM set-up highlighting the key complementary properties assessed by both AFM and confocal laser scanning microscopy inset. Created with BioRender.com

useful for understandi/ng health, disease, and treatment efficacy. For instance, Targosz-Korecka *et al.* (2017) demonstrated the degradation of the cellular glycocalyx in diabetes correlates to disease progression, as did the stiffening of endothelial cells in a mouse model.[27] In chemistry-driven fields, such as nanomedicine, AFM is currently being utilized to answer a number of interesting questions, shedding light on the fouling of nanomaterials *in vivo*, the functionality of targeted materials, and detecting cellular changes relevant to diagnosis and treatment. In large part, the expansion of AFM into the preclinical sphere is owed to the described advancements in technology and the availability of diverse probe labelling and sample preparation strategies.

Attachment Chemistry

Tip Functionalization Strategies

In single-molecule recognition experiments, the interaction between the ligands tethered on the AFM tip and the receptors on the surface (or vice versa) is interrogated by applying an external force to the complex, until the bond ruptures at a measurable unbinding force. The literature is replete with various strategies to suitably functionalise surfaces with proteins, hydrocarbons, antibodies, nanoparticles, etc. via covalent bond formation or simple physisorption. For reciprocal interaction to take place, not only should the biomolecules retain their native conformation and functionality, but the bond between them and the inorganic substrate should be stronger than the intermolecular forces involved in the complex formation. As highlighted elsewhere (*e.g.* Müller et al., 2020),[3] advancements in cantilever design and tip functionalization have been a great boon to exploring biomolecular interactions. Significant research towards chemical attachment strategies has enabled scientists to tether probiotic bacteria to AFM probes for quantifying forces that drive cell-cell and cell-substrate interaction.[28] In principle, the tip of the cantilever is replaced with a living cell guided by specific ligand-receptor pairs, non-covalent interactions or chemical fixation strategies. Through decorating the cantilever with various molecules or nanoparticles, it is possible to explore the native chemistry of surfaces and membranes (**Figure 4**). In brief, common mechanisms for grafting of molecules on inorganic substrates are listed below (**Table 1**).

Table 1: Common Classes of Probe Attachment

Class of Probe	Frequently Used Strategies	Reference(s)
Small molecule	SAMs. Click reaction	29–32
Nucleic acids, oligosaccharides	Hydrazide coupling	33
Antibodies	Click reaction, hydrazide coupling	33
Protein and peptides	Tris-NTA, aldehyde and maleimide linkers, enzyme-assisted, *eg.* Sortase A	34–36
Virion	Heterobifunctional PEG linker	37,38
Bacterium	Polydopamine coated colloidal probe, electrostatic (PEI), covalent (APTES), polyphenolic proteins (Cell-Tak)	39–41
Whole Cell	Integrins, Concanavalin A	5

Linker Chemistries

Among the driving forces of advances in single molecule imaging of samples is the availability of a wide array of linkers, and methods for attachment to the cantilever (**Table 2**). Although PEG linkers remain the most common due to their history and commercial availability, alternative linkers with intriguing capabilities have begun to filter into wider usage. One of the advantages to developments in linker chemistry is that each linker possesses a unique chemical signature observable in the retrieved data. Moreover, the use of cleavable linkers in combination with live cell AFM has been of great benefit for observing entry and trafficking behaviors of single biomolecules, viruses, and other exogenous entities after the assessment of their non-covalent bond formation with elements of the cell surface e.g.: receptors. As discussed by Viljoen *et al.* (2021),[5] common strategies for attaching components to the linker include aminosilanized cantilevers in co-ordination with heterobifunctional PEG linkers, self-assembled monolayer formation on gold cantilevers, click chemistry approaches, and enzyme assisted tip modification.

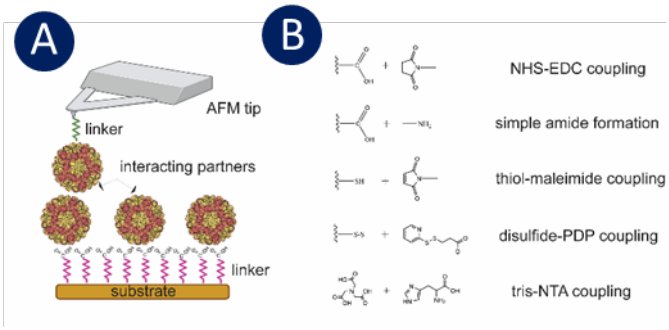

Figure 4: Common attachment chem str es, **(a)** bas c set up of a con /ent ona AFM exper ment on a mode surface, probe mo ecu e s attached to the AFM cant e /er *via* a nker, and used to assess b omo ecu es bound to a substrate a so by /ay of a linker molecule. **(b)** S mp e coup ng chem str es used to attach agents to linkers on the tip or substrate. NHS-EDC: N-hydroxysuccinimide-1-Ethyl-3-(3-d methy am nopropy)carboq m de,disulfide-PDP:disulfide-pyridyldithiopropionate, tris-NTA: tris-Nitrilooacetic acid. Created with BioRender.com

Moreover, advances in unnatural amino acid incorporation into peptides and proteins and thus introducing functional handles *eg:* azides and strained alkynes, that do not exist in physiological environments, allow for site-specific attachment and controlled orientation of single molecules; often through simple clickable reactions. For smaller proteins and peptides this approach is preferable to common N-Hydroxysuccinimide (NHS) and isothiocyanate chemistries which can generate random orientations, destabilize secondary and tertiary structures, and interfere with binding through steric hindrance or attachment to key components involved in non-covalent bond formation. Each attachment chemistry and linker needs to be carefully selected for the desired application, for example, control over orientation is less important for larger entities such as viruses, as their icosahedral symmetry means that binding behaviours will likely be unimpeded by random attachment strategies such as NHS; whereas enzyme degradable linkers may be useful for studying specific interactions, however if the enzyme is secreted extracellularly, this may confound obtained results.

Table 2: Common linkers used in tip modification

Linker	Main Benefits	Reference(s)
Poly(ethylene) glycol	Molecular fingerprint to detect specific adhesion events and imparts conformational mobility	[3,42]
Photoactivable linkers	Conformational switching with different 'on' and 'off' states	[29]
Peptides	Enzyme degradable motifs can be built into sequence, fixed orientation, higher cell-adhesion events	[43]
Complex Linkers	Can impart distinct unfolding signatures through incorporation of specific motifs	[44]

Nanoparticle Modification

CFM measures adhesion and/or friction forces between chemically functionalised AFM tips and samples. Although CFM provides molecular level resolution, it is limited by the stability of the organic moieties on surface. Since both interacting partners should participate in thousands of FD cycles, the grafting of molecules of interest becomes a key determinant in the extraction of thermodynamic and kinetic parameters. An alternative approach to directly linking molecules to the cantilever, is to employ nanoparticles (NPs) which are subsequently adjoined to the tip either chemically or through physical entrapment. Commonly, silicon and gold nanoparticles are utilized for this purpose due to their surface chemistry being available for silanol and thiol coupling respectively. Despite the fact that reactions forming covalent bonds (i.e., S-Au, or Si-O) are extremely facile, the fact they have a high risk of cleavage reduce their lifetime on the AFM tips. Towards this end nanocrystalline diamond (NCD) tips with high mechanical stability have been reported. By subjecting hydrogen terminated NCD tips to a photochemical reaction at 254 nm, long chain acids could be tethered via the formation of a C-C bond.[45]

The increased use of NPs in commercial products has led to adverse physiological effects because of their ability to cross biological barriers. The study of particle-cell interaction is important in determining the fate and transport of NPs and also aids research in the field of NP based theranostics. Industrially relevant engineered NPs of cerium and iron were attached on AFM tips and the forces between the tip and lung epithelial cells were measured under physiological conditions.[46] By using a silica sphere of 3.5 µm radius positioned on the AFM tip the colloidal stability as a function of the attractive Van der Waal's force and repulsive electrostatic forces (also known as a double layer force) was examined. In this semantic work, the stability of colloidal silica NP was studied by measuring the interaction forces between the NP and flat silica surface in aqueous sodium chloride solution. In order to construct AFM tips with a single NP at its apex, ceria NP of ~50 nm diameter was attached to a standard pyramidal silicon nitride probes using an epoxy glue. Using these ceria NP terminated tips, acidity-dependent adhesive forces between the tip and flat silica surface were measured.[47,48]

Due to the complex nature of most biomolecules, many examples contain amino acids with groups naturally able to participate in these coupling reactions, e.g. cysteine and methionine. Nanoparticles also grant the capacity to be used in conjunction with techniques such as Fluid-FM, wherein the nanoparticle is held in place on the tip apex via a microfluidic channel with negative pressure applied.

Immobilization of Biomolecules on Model Surfaces

Much as with linker chemistry, the diversification of attachment strategies for the immobilization of molecules on model surfaces has allowed for vast improvements in the retrieval of important structural and chemical information of biomolecules. Due to improvements in attachment chemistry for surface preparation, the high resolution of AFM can be used to assess structural biology and identify oligomerization states of proteins and biomolecules at the nanoscale. The surface density of biomolecular partners on substrates are optimized to create a single-layer of receptors to achieve significantly observable-binding probability. In SMFS, the goal is to maintain the binding probability low to favor single-bond rupture events that allow extraction of kinetic and thermodynamic parameters. It is important to note that too high ligand density can impede the single-molecule level of probing between the interacting partners. By following a mixed monolayer strategy, problems arising from biomolecular overcrowding can be circumvented.

Biomedical Applications of AFM

Owing to the strengths and developments outlined, it is clear that AFM has the potential to explore pertinent questions in the biomedical sphere, yielding molecular-level insight into

physiological phenomena, *e.g.* supramolecular bond formation in receptor-ligand interactions. Among the common uses of AFM for exploring biological processes in our laboratory, are for assessing the distribution of important molecules at the cell surface, examining the mechanical properties of biological samples, and exploring binding and entry mechanisms of important biomolecules and pathogens.

Exploring Cell Surface Organization

The role of cell surface interactions is crucial for the vast majority of cellular functions and behaviours. The intricate interactions at this interface dictate the delicate interplay underlying physiological and immune functions, which are often dramatically altered in pathological conditions. Small changes in lipid chemistry,[49] receptor expression,[50] and organization of the cell surface[51] can have incredible ramifications for health and disease through the downstream behaviours exhibited by cells and tissues. Increases in polar lipid concentration can be a sign of cancerous behaviour,[52] availability of important binding domains can alter cellular function,[53] and the expression of intercellular junction proteins can wildly alter the composition and tensile strength of tissues.[54,55] In the case of pathogenic microbial cells, alterations to surface chemistry could be the difference between successful parasitism or replicative failure. Due to the ability to assess interactions at nanoscale resolution, AFM is uniquely poised to provide molecular insights into important processes in homeostasis and disease.[5] In particular, a great strength of AFM is the ability to spectroscopically probe the chemistry of cellular surfaces and interfaces, identifying the topography of important domains, and the distribution of important biomolecules.

The topography of membrane constituents plays an integral role in cellular behaviour and interactions with physiological processes. The arrangement of membrane motifs can alter receptor expression patterns,[56] cellular stiffness,[57] internalization pathways,[58] and play a role in cancer cell migration.[59] Thus, identifying patterns in the chemistry of the cell surface is a vital point of study in our group and others. Through probing the surface of living cells with selected chemical motifs or biomolecules and monitoring binding forces while the tip scans the cell surface, the adhesion map data can be used to identify locations where chemical species or biomolecules of interest are distributed (**Figure 5**). This information is key to driving our understanding of cellular function towards a molecular and chemical level.

Through attachment of hydrophobic functionalities, such as a terminal methyl group (CH_3) to the tip of the cantilever, it is possible to survey cell surfaces and identify the hydrophobicity of various domains within the exposed membrane of mammalian cells and bacteria.[5,60] Using CFM, this approach allows for quantification of the interactions within the contact region (~5 nm^2), which typically features ~25 functional groups with which the probe can interact (**Figure 6a**).[61] As the cantilever raster scans the surface, attraction and repulsion of the tip (**Figure 6b**) are monitored as the probe encounters regions of hydrophobicity or hydrophilicity respectively, with the CH_3 group either engaging in establishing a hydrophobic interaction or being repelled by the local environment (**Figure 6c**).[60,61] This is critical for the adhesion of biomolecules that rely

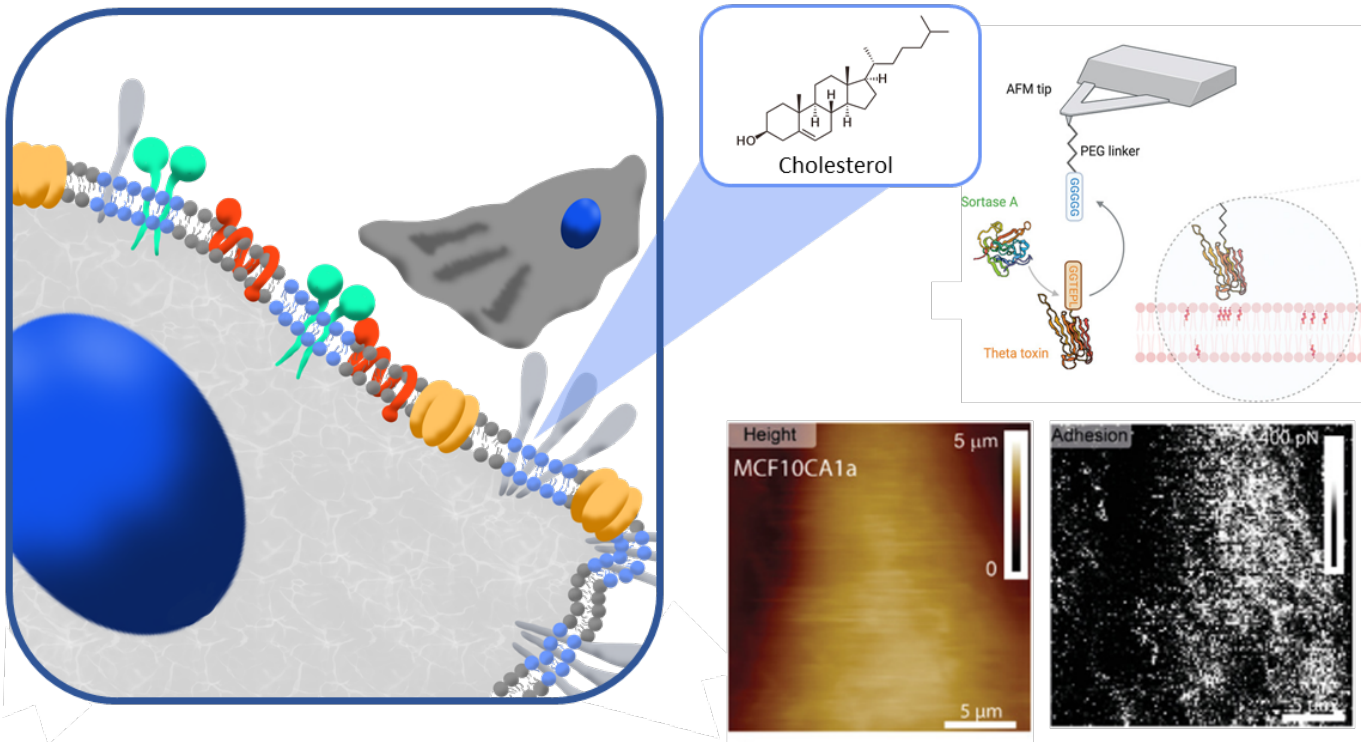

Figure 5: Cell surface organisation assessed by AFM. Example of an application of a site-directed coupling method (top left) reaction to assess the distribution of cholesterol within the complex surface of the plasma membrane of cells (right). Example images (bottom left) showing the shape of the cell (height) and the adhesion map (adhesion) indicating the presence of cholesterol within the membrane. Figure adapted in part from Dumitru *et al*. *Adv. Sci.*, 2020, **7,** 2002643. copyright © Dumitru *et al.* (DOI: 10.1002/advs.202002643).

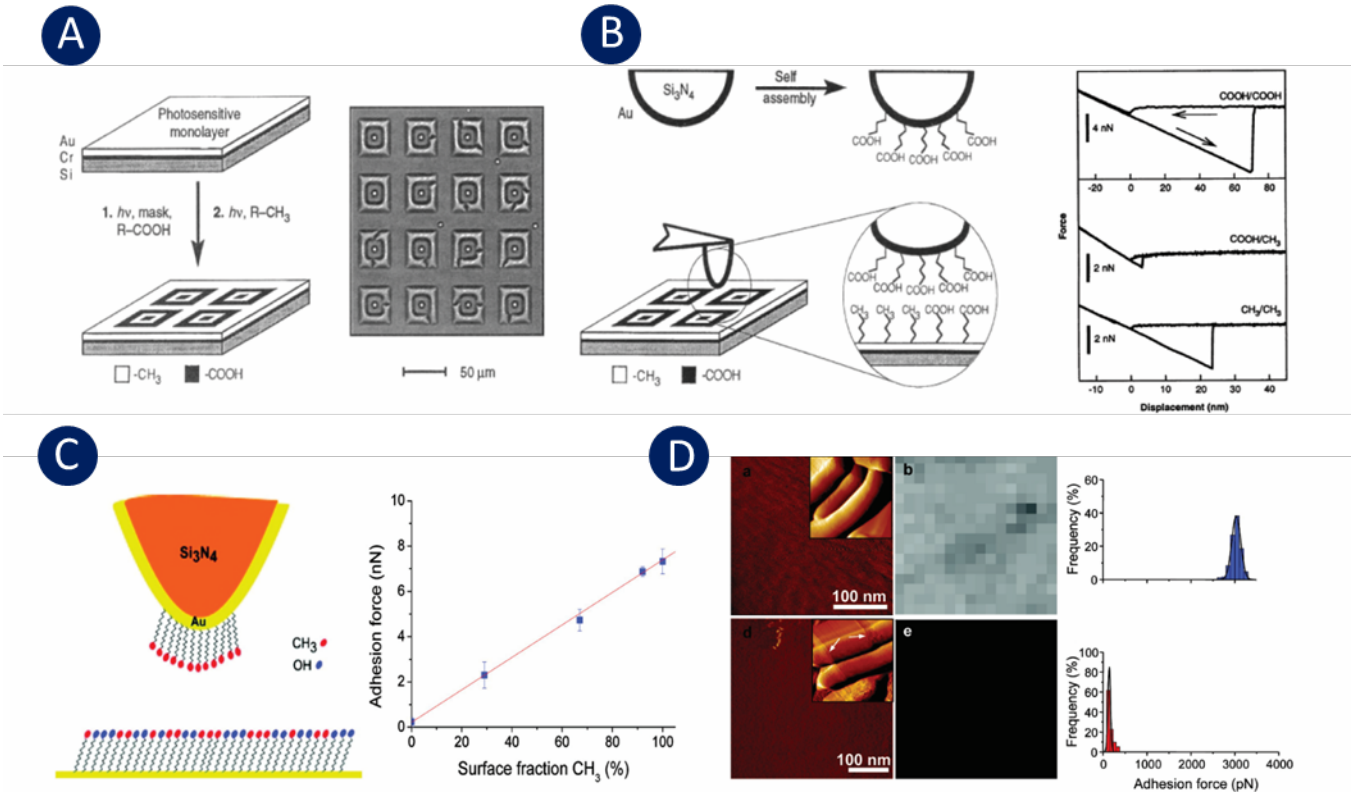

Figure 6: Chemical force microscopy for assessment of hydrophobicity of surfaces and membranes. **(a)** generation of model surfaces and tip functionalisation for assessment of CFM detection of chemical motifs. **(b)** examples of retrieved curves when the probe interacts with a purely hydrophilic region (top), and even mix of hydrophobic and hydrophilic components (middle) and a purely hydrophobic zone (bottom) of the surface. **(c)** assessment of the proportionality of hydrophobic:hydrophilic surface groups. **(d)** Use of CFM to assess the surfaces of live single cell fungi before (top) and after (bottom) removal of hydrophobins, showing that binding forces are related to the presence of these cell wall components. Figure adapted from Dague *et al., Nano Let.*, 2007, **7**, 3026-330. copyright © Dague *et al.* (DOI: 10.1021/nl071476k).

on hydrophobic interactions either for initiating binding or permeation of the membrane, *e.g.* fungal hydrophobins.[60] Hydrophobic interactions are frequently a key feature of adhesion for many pathogenic fungi and bacteria. In the case of *Aspergillus fumigatus,* the coordinated effort of the functional groups assessed was demonstrated to reach adhesive forces >2.9 nN, whereas after removal of the cell wall (specifically rodlets and hydrophobins), the attraction of the cantilever dropped significantly, yielding forces <0.35 nN (**Figure 6d**).[61] Through comparison with model surfaces, the retrieved values for these domains suggests that the conidial surface corresponds to approximately 15 methyl and 10 hydroxyl groups per pixel.[60] Confirming that these domains, and hydrophobic interactions more generally, likely play a key role in adhesion and pathogenicity of *A. fumigatus*.[60] This technique and similar, have now been applied to other pathogenic fungi and bacteria, suggesting that these relatively simple interactions are conserved as a mechanism for pathogens to attach to surfaces and cells.[62]

As highlighted by research with microbial pathogens, identifying where phenomena tied to hydrophobic interactions may take place is very useful information, and understanding the underlying chemical composition of such regions is likewise of great import. Expanding on this approach to assessing membrane characteristics, recently we have focused on identification of changes in the lipid chemistry of the plasma membrane's outer leaflet in healthy and diseased cells, including red blood cells (RBCs)[63] and breast cancer cell lines.[57] Cholesterol-rich lipid rafts often serve vital roles for vesicular budding[58] and the recruitment or exclusion of receptors, integral membrane proteins, and transporters.[64] In cancerous cells changes in the lipid composition and chemistry have been tied to oncogenesis.[59] Cholesterol in particular is able to covalently modify specific proteins involved in tumorigenic signaling *e.g.* hedgehog family proteins.[65,66] Moreover, increased biosynthesis and uptake can lead to the formation of specialized microdomains favourable to hyperactivation of signaling pathways.[67] Given the importance of cholesterol homeostasis in health and disease and its ties to specific distribution patterns, AFM is an excellent tool for the assessment of changes in cell surface lipid composition.[68] As several bacterial toxins are known to target specific lipid species, it is possible to implement these proteins, or fragments there-of, to chemically profile the lipid content of the cell surface.

Through the attachment *Perfringolysin O* (θ) toxin to the cantilever *via* Sortase A enzyme assisted tip functionalization, specificity for cholesterol is imparted due the D4 region of the protein interacting with the hydroxyl group at the position 3 of cholesterol,[69] granting the ability to assess the nanoscale distribution of the lipid across the surface of the plasma membrane. The enzyme assisted functionalization provides

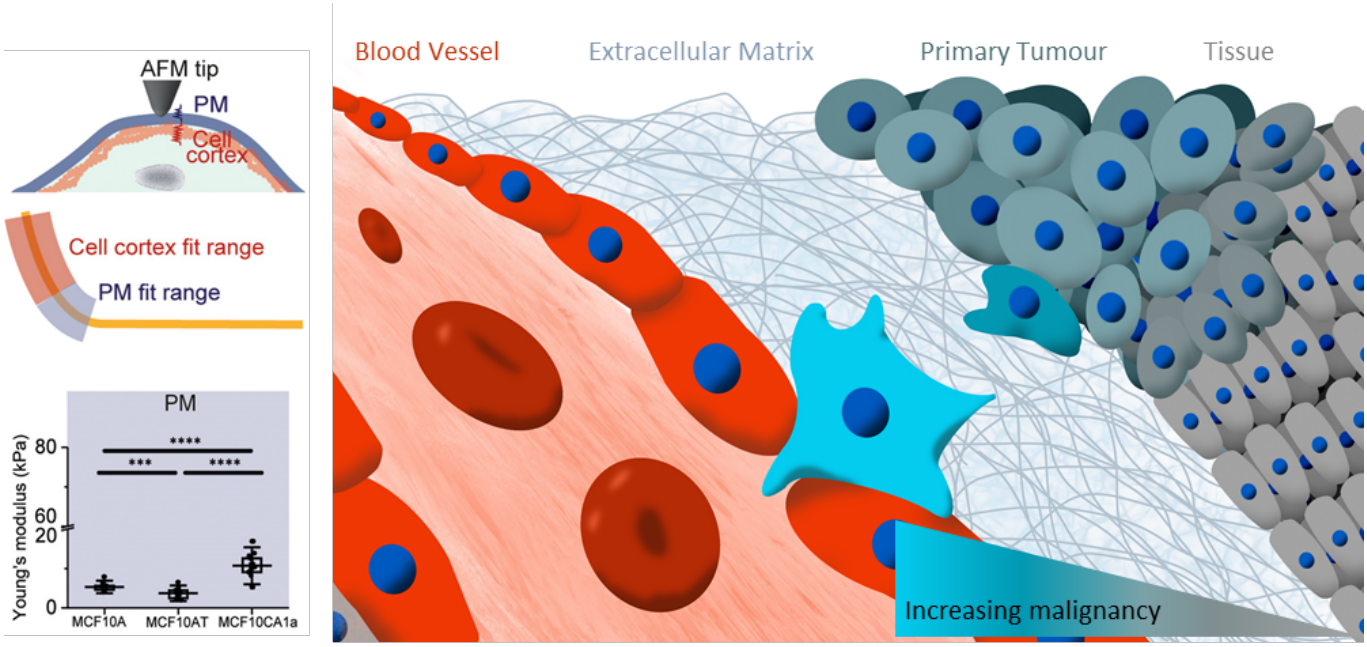

Figure 7: Biomedical significance of assessing cell elasticity and mechanical properties. Using the force of the AFM tip (top left) it is possible to recover the elastic properties of assessed curves (middle left) and compare across cells (results from breast cancer cell lines of increasing malignancy, bottom left). This mechanical property being related to the capability of malignant cells to navigate important barriers, such as through endothelial junctions and through extracellular matrix, allowing for spread from the original tumour (right). Figure adapted in part from Dumitru *et al. Adv. Sci.*, 2020, **7**, 2002643. copyright © Dumitru *et al.* (DOI: 10.1002/advs.202002643).

controlled attachment to an inserted motif at the *N*-terminus, ensuring the orientation and availability of the probe for binding. In addition to detection of cholesterol, we have utilized lysenin toxin chelated to the tip *via* His-tag Ni^{2+} NTA chemistry to explore the distribution of sphingomyelin in surface membranes.[68] Using these probes, we have been able to characterize the distribution of cholesterol and sphingomyelin on surfaces at high resolution[68] and demonstrated that the localization of such species is important for the behavior and function of living cells.[63] For instance, by exploring the lipid chemistry and distribution of cholesterol within the outer leaflet of cancerous cells, we have reported that significant differences exist between breast cancer cell lines of different malignancy and invasiveness.[57] Across a suite of MCF10 cell lines, we found that the proportion of cholesterol was greater than 20% of the surface for the metastatic variation (MCF10CA1a) whereas in the less malignant (MCF10AT) and premalignant (MCF10A) variations this proportion decreased significantly, being approximately 5 and 10 % of the surface respectively, indicating that AFM can provide useful label-free insights into cancer progression and lipid homeostasis.[57]

Related to the chemical composition of the surface membrane, the availability and organization of receptors and other biomolecules at the cellular surface is a non-trivial matter. The aggregation state, conformation, and positioning of surface molecules play important roles in determining the formation of supramolecular bonds.[53] The ability of surface proteins and molecules to participate in bond formation and the nature of these bonds has significant ramifications for cellular behaviours such as adhesion, migration, and signaling. Through probing non-covalent bond formation with a ligand or biomolecule of interest, it is possible to characterize the distribution of surface receptors, identify their upregulation or downregulation, and glean insight as to whether differential binding states occur which could indicate conformational differences in surface proteins relevant to discerning important putative partners.[5]

In Dumitru *et al*. (2020),[70] we explored the behaviour of human G protein-coupled C5a Receptor (C5aR), using affinity imaging to detect orientation of the protein in lipid membranes and identifying, for the first time, a cooperative binding mechanism likely tied to its function. Given the receptor's role in chemotaxis,[71] inflammatory responses,[72] cell activation,[73] and links to inflammatory pathologies,[74,75] Alzheimer's disease,[76] and cancers,[77] understanding the molecular binding behaviours and functioning of C5aR is important for the development and application of therapeutics. Using a combination of FD-AFM and molecular simulations, we identified for the first time an allosteric two-step binding process occurring at separate positions within the structure.[70] The ability to probe such important interactions and profile surface distributions of receptors is important for understanding pathology and is rapidly becoming key information for the rational design of treatments.

Assessing Cellular Mechanics

In addition to performing high resolution images capable of identifying distribution of chemical species and important macromolecules at the cell surface, AFM is a powerful technique to probe mechanical properties of living cells and to map the spatial distribution of their cell mechanical properties (**Figure 7**).[78] This capability being able to provide indirect information about the organization of the cell cytoskeleton. As such, AFM has been involved in the general understanding of cell mechanosensing in both normal[79,80] and pathological states, [5] especially cancers. A key hallmark of cancerous cells is that many of their endogenous features depart from those of

their tissue of origin, from their gene expression through to their morphology. AFM is a uniquely positioned tool to assess the physical alterations, being capable of detecting changes in stiffness, topography, receptor expression,[5] and when combined or correlated with other techniques, how these features interact with intracellular mechanics.[37] This is pertinent to improving our understanding of the specific behaviours of select cancers,[57] the mechanobiology of cancerous cells and tissues, transition between healthy tissue and cancerous states, and identifying novel therapeutic targets. Information regarding the elasticity of cells often correlates to either chemical composition of the cellular glycocalyx and outer membrane, or to underlying features within the cytoplasm, *e.g.* the cytoskeleton. The changes in these features being required for metastatic cells to navigate complex 3D environments such as tumour ECM and spread. By combing AFM with other mechanical assays to apply dynamic force regime to cells, Andreu *et al*. (2021)[81] recently demonstrated that increasing loading rates trigger talon-dependent mechanosensing, leading to adhesion growth and reinforcement, and YAP nuclear localization. Multifrequency AFM imaging has been combined with recent gains in imaging speed through application of small cantilevers to obtain high-speed scanning AFM.[23] Recently, Rigato et al. (2017)[82] developed high-frequency microrheology experiments to probe the viscoelastic response of living cells from 1 Hz to 100 kHz. They demonstrated that benign and malignant cancer cells exhibit different scaling laws at high frequencies, providing a unique mechanical fingerprint. Other groups have shown that AFM can play a key role in deciphering the role of cell mechanics in pathologies. For instance, LeClaire *et al*. (2021)[83] have evidenced that the use of biomechanical fingerprinting of single nanoscale small Extracellular Vesicle (sEV) provides an attractive method to detect alterations in parental cells, such as during malignant transformation. By comparing the structure and mechanical properties of breast cancer cell-derived sEV and secreting cells, they revealed that sEVs show reduced Young's modulus concomitant with a decrease in cell stiffness as cells progress from nontumor to noninvasive to invasive breast cancer phenotypes.[57,83] These findings matching recent work within our own laboratory,

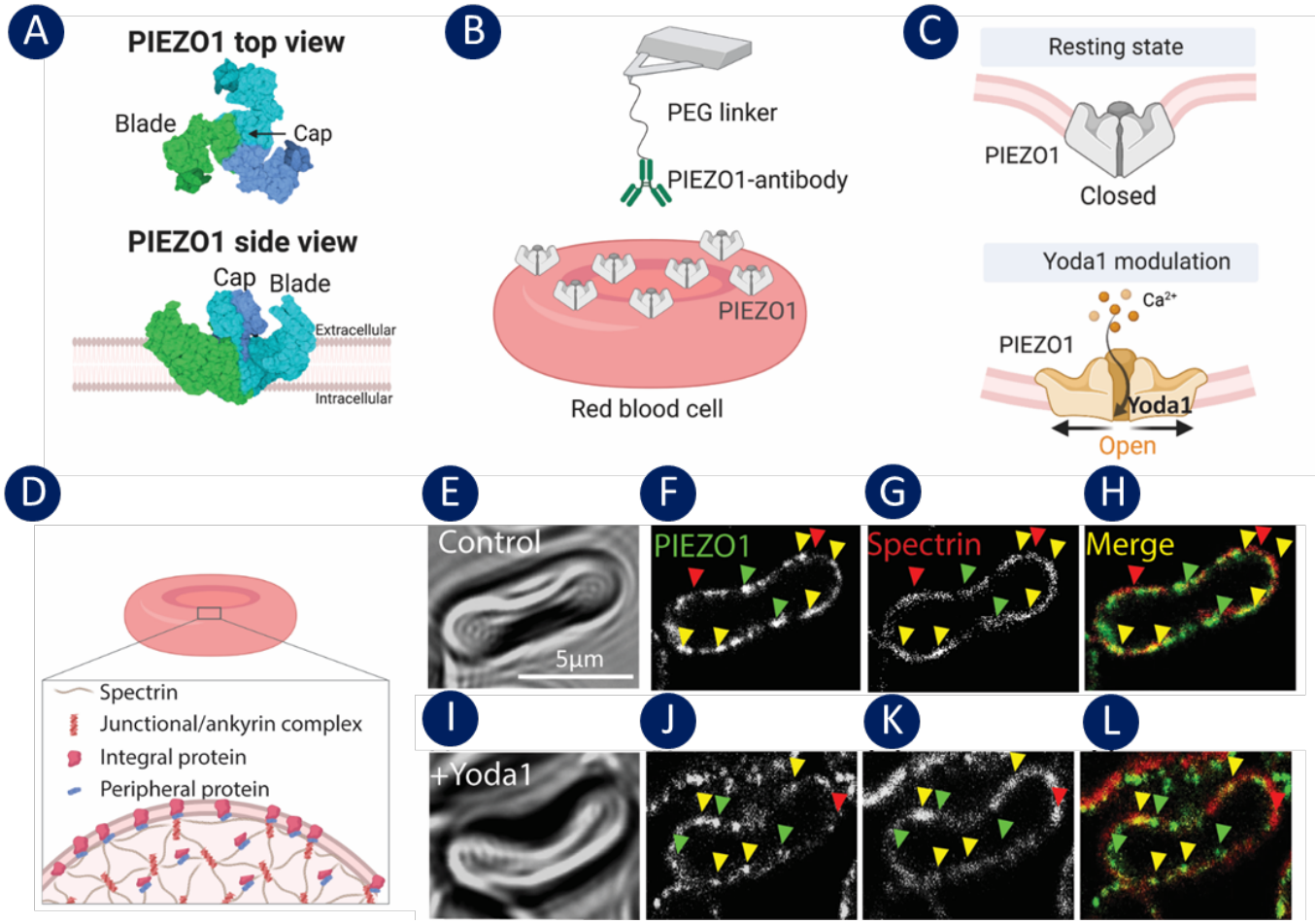

Figure 8: Cell mechanics contribute to the performance and function of PIEZO1. **(a)** Structure of the PIEZO1 complex as seen from the top and side the latter embedded within the plasma membrane, showing the cap and blades required to undergo conformational change in order to act as a transmembrane transport for Ca^{2+}. **(b)** AFM set up used to probe PIEZO1 conformation and behaviour on live red blood cells. **(c)** Proposed mechanism of function, activation by Yoda1 resulting in changes in membrane stiffness and surface tension, encouraging PIEZO1 to switch from the resting (top) to open configuration (bottom). **(d)** Underlying spectrin network of red blood cells, which controls surface properties such as curvature and elasticity. **(e-l)** Confocal images of live red blood cells showing the distribution of PIEZO1, brightfield of control cell **(e)** and Yoda1 activated cell **(i)**, the localization of PIEZO1 **(f** & **j)** and spectrin **(g** & **k)** for both cells, co-localization of signals is shown in figures **h** & **l**. Figure reproduced from Dumitru *et al.*, *Nano Lett.*, 2021, **21**, 4950–4958. copyright © Dumitru *et al.* (DOI: 10.1021/acs.nanolett.1c00599).

wherein we demonstrated that similarly these changes in elasticity can be linked to the changes in cholesterol[57] and glycan[84] distribution described previously. In addition, recent works have shown the possibility to decipher properties of plasma membrane and cell cortex by probing mechanical properties of living cells with AFM. In Dumitru et al. (2020),[57] we illustrated that cancer cells have drastic changes in its composition, organization and mechanical properties. The altered membrane composition under cancer progression, as evidenced by plasma membrane-related cholesterol levels, leads to a stiffening of themembrane that is uncoupled from the elastic cytoskeletal properties. Conversely, cholesterol depletion of metastatic cells leads to a softening of their PM, restoring biomechanical properties similar to nonmalignant cells.[57]

Among the details examined by our group and others, is the role of assessed features in relation to mechanical properties and the behaviours exhibited. In RBCs the mechanical properties of the plasma membrane alters the ability of membrane proteins to participate in binding and bond formation, as we have illustrated with the ion channel, PIEZO-1 (**Figure 8a**).[53] In Dumitru *et al*. (2021),[53] we demonstrated that the localization, conformation, and abundance of the PIEZO-1 on the surface of RBCs is tied to modulation by Yoda1 in conjunction with curvature and membrane tension. Using a PIEZO1 antibody targeted to the cap component of the assembled membrane channel on live RBCs (**Figure 8b**), we were able to assess whether the complex was in the resting state or open (**Figure 8c**).[53] In order for PIEZO-1 to function it needs to enter the open state, which was correlated with changes in lipid distribution and stiffness, which were detected with AFM and correlated to alterations in the spectrin network (**Figure 8d**).[53] These results suggest that the morphological and underlying cytoskeletal architecture changes modulated by Yoda1 are requisite for optimal performance of PIEZO-1 (**Figure 8e-l**). This was not only the first time that the spatial distribution was imaged in high resolution, but combined with the mechanical properties and confocal imaging, we were able to propose a mechanism for the behaviour of PIEZO1. Altogether, these recent findings highlight the potential of AFM to improve our understanding of human health and diseases from a mechanical standpoint,[85,86] while highlighting the ability to aid in developing new diagnostic and therapeutic options in the future.[87,88]

Molecular Dynamics of Cell Binding & Infection

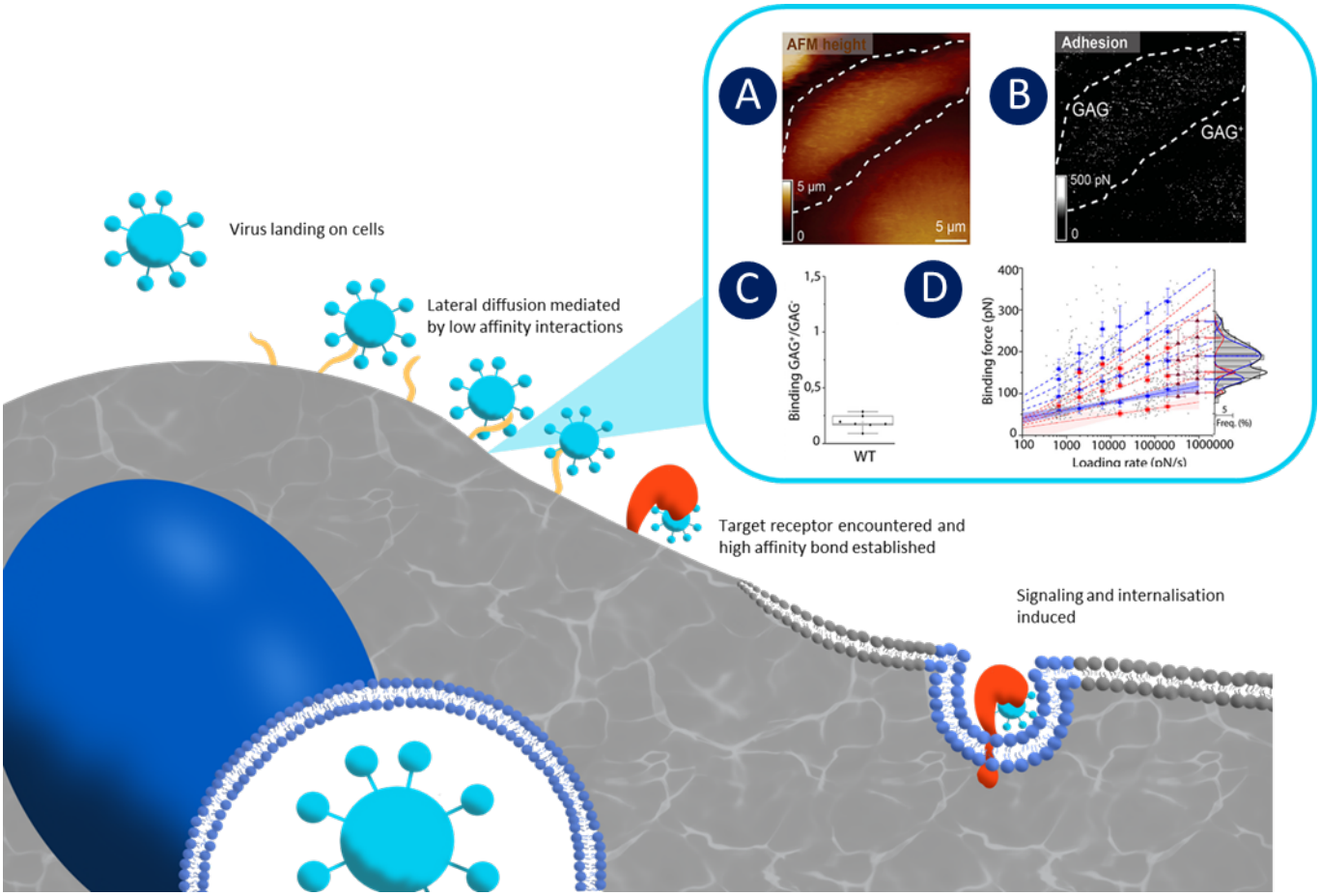

Figure 9: Binding and entry behaviours of viruses when interacting with a cell. Process of viral entry from binding from initial interactions with surface molecules leading to endocytosis. Example of binding information demonstrating both low and high affinity interactions from Delguste *et al*. (2020) **(inset)**, showing that from using AFM to image the surface of cells **(a)** adhesion data can be retrieved **(b)** showing both high (GAG) and low (GAG-) affinity interactions. Overall displaying a low binding probability **(c)** but distinctly divided into separate interactions when assessed quantitatively **(d)**. Figure reproduced in part from Delguste *et al*., *Nano Lett*., 2020, **21**, 847–853. copyright © Delguste *et al.* (DOI: 10.1021/acs.nanolett.0c04609).

Among the key capabilities highlighted in this review, the ability of AFM to examine binding strength, receptor affinity and determine the physical interactions between pathogens and their molecular targets is of great importance for biomedical applications. Binding and entry into host cells is a complex multi-step process, often featuring many components working in concert that facilitate adhesion to the cell surface and hijacking of endocytic machinery (**Figure 9**).[89] Through decorating either the cantilever or a nanoparticle with bacteria, viruses, or their component proteins, it is possible to explore the formation of supramolecular bonds and study these interactions in great detail.[5] Through the application of SMFS, we are able to probe binding of ligands such as capsid elements down to the level of a single non-covalent bond, and in conjunction with model fitting, is a powerful tool for distinguishing multivalent interactions.[5] These supramolecular bonds being the keystone of pathogenesis, thus understanding their formation is important for understanding the native behavior of infectious agents, identifying druggable targets, and evaluating therapeutics. In collaboration with others, we have contributed to the understanding of other classes of pathogen,[90–93] however, for the purposes of this feature, we will focus on viral interactions.

Among the key strengths of our group is the ability to assess the binding interactions of viruses with specific receptors and ligands.[94] Reovirus is a particularly interesting case, as while usually an asymptomatic infection,[95] many reoviruses demonstrate excellent oncolytic properties.[96] The replication of many strains being tied to the expression of pathways commonly upregulated in cancerous cells (*e.g.* ERK signaling).[97] Due to these factors select strains of reovirus are being examined intensively for use in cancer therapies. However, among the limitations, little is known regarding the native binding and entry mechanisms of these viruses. As such, understanding the supramolecular chemistry of reoviruses required for efficacious functioning is of great importance for establishing them as safe and viable therapeutic treatments.

As is the case with many viruses, reoviruses possess a complex interplay between their capsid proteins and surface biomolecules of the host cell. In particular, the σ-1 spike protein appears to mediate a number of interactions. Recently we have demonstrated that the conformational flexibility of this protein is tied strongly to the selectivity, affinity, and avidity exhibited when binding to surface molecules (**Figure 10**).[38,89,98] We have shown that this viral element establishes multivalent bonds with the intercellular junction protein JAM-A,[89] while the avidity of these interactions being related to the conformation of both the target receptor and the capsid protein.[38,89] In the case of reovirus' interactions with integrins, improved binding has been observed in response to the addition of Mn divalent cations, favouring the high-affinity state of β1 integrins.[89] Through the substitution of amino acids at select points within the σ-1 sequence to modify conformation, we have strikingly evidenced that interactions with JAM-A can be improved or weakened depending on the conformation in which the spike protein is locked.[98] For instance, a mutation in the head of the protein confers an increase in both valency and binding affinity, with significant improvement to association rate, decrease in disassociation rate, and higher binding frequency.[98] Further, in Kohler *et* al. (2019), we have shown that sialic acid (SA) interacts with the σ-1, inducing a conformational change that improves receptor binding. While previously glycan binding was often considered a simple tethering interaction, in the T3 strain, SA binds to a specific domain within the σ protein, being able to withstand forces between of 25-400 pN.[38] This interaction induces the extended conformation of the spike protein, potentially through the cis-trans isomerization of a gly-pro peptide bond adjacent the SA binding pocket, increasing its binding availability and adhesive properties.[38] Using combined confocal-AFM, we were able to correlate increases in binding to

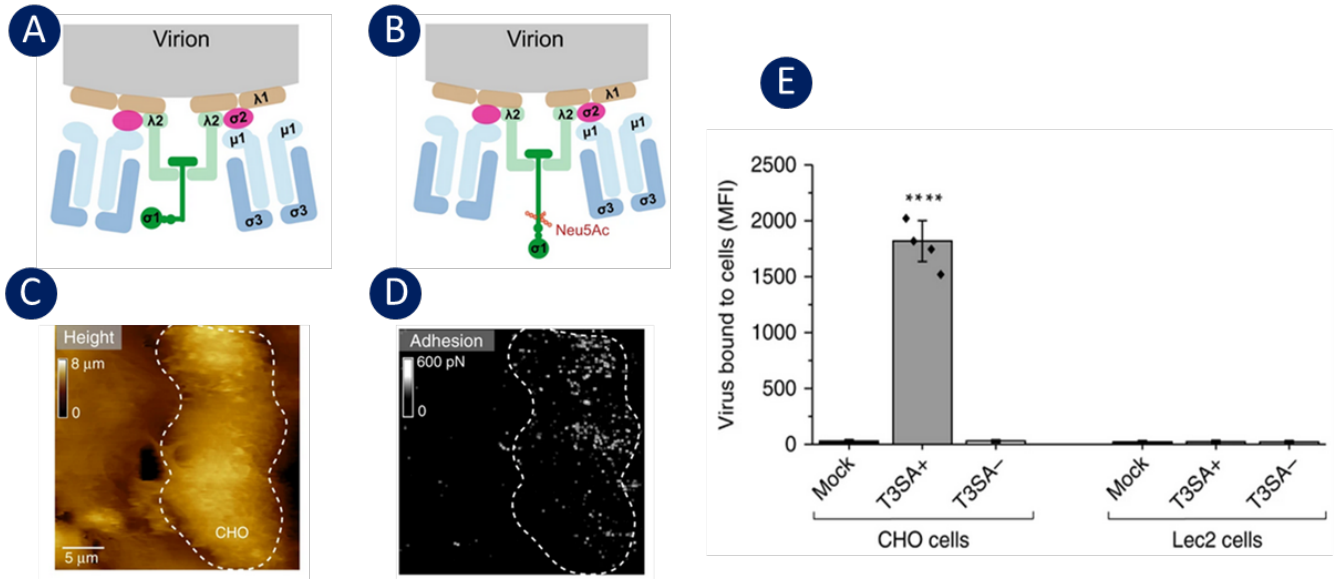

Figure 10 Conformation related binding behaviours of reovirus **(a)** The presence of sialic acid (Neu5Ac) induces the extended conformation of the σ-1 capsid protein **(b)**. This allows for improved binding to a target receptor, in this case JAM-A. When probing as a sialic acid positive and negative co-culture (height image in **c**) the adhesion of a specific strain (T3SA+) susceptible to this phenomena **(d)** is observed. Whereas this is not the case for a strain unable to undergo this transition (T3SA-) or when probing cells that lack sialic acid **(e)**. Figure adapted from Koehler *et al.*, *Nat Commun.*, 2019, **10**, 4460. copyright © Koehler *et al.* (DOI: 10.1038/s41467-019-12411-2).

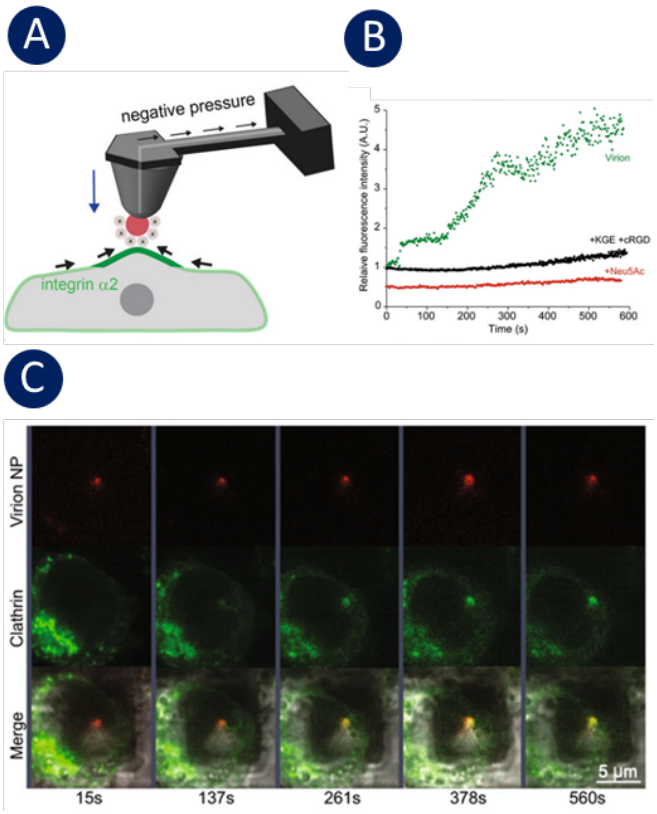

Figure 11 Results of a clathrin recruitment experiment. When a virus or coated nanoparticle is held in place for Fluid-FM and brought into contact with a clathrin-GFP cells **(a)**, an increase in GFP fluorescence can be seen **(b)**, and over time fluorescence signals from the probe and the reporter protein begin to co-localise. Figures adapted from Koehler *et al.*, *Nat Commun.*, 2019, **10**, 4460 and Yang *et al.*, *Adv. NanoBiomed Res.*, 2021, **1**, 2100077. copyright © Koehler *et al.* (DOI: 10.1038/s41467-019-12411-2) and Yang *et al.* (DOI: 10.1002/anbr.202100077)

improvement in the recruitment of endocytic machinery (specifically clathrin), indicating that the formation of these bonds is directly involved in the activation of important entry pathways (**Figure 11**).[89] Interestingly, a combination of these factors and expression of sialylated glycans allows for the T3SA+ strain to better infect malignant breast cancer cells.[84] Given the importance of glycan binding for many viruses and the development of cancer virotherapies, in Mohammed *et al.* (2021),[84] we evidenced improved binding of reovirus to malignant breast cancer cells is related to the expression of certain glycans at the cell surface. As the malignant cells express different glycosylation patterns on the cell surface,[84] this inherent feature could boost the utility of reovirus treatments such as Reolysin®.[99] As we continue to uncover more of the mechanics and functioning of reovirus, this information can be directly utilised to improve binding of variants used in clinical trials for cancer therapy and vaccination.

To further highlight the complicated nature of viral binding and the important link to supramolecular chemistry, in Delguste *et al.* (2018),[100] we have illustrated that glycan-binding is critical in the early stages of γ-herpesvirus infection. However, the valency of the glycan binding interactions is controlled by the capsid proteins, being negatively regulated by gp150.[100] By limiting the valency and reducing avidity through lowering the number of bonds formed upon virions landing on the cell surface, counter-intuitively infection can be mediated either through lateral diffusion to encounter a stronger affinity receptor, or the virion may be released from the cell surface in order to invade a more appropriate host cell.[100] The results of AFM investigations correlated with infection studies, where-in despite more binding of gp150$^-$ virus to host cells, rate of productive infection did not improve.[100] Moreover, heparin injections can be utilised to block cellular binding.[100]

Among the biomedically useful information that can be garnered *via* the suite of AFM techniques, therapeutic molecules can be assessed and screened rapidly. For instance, blocking of receptor interactions through the prior binding of antibodies, fragments, and peptides. Recently in Yang *et al.* (2021),[101] we demonstrated that after enzymatic processing the rotavirus VP8* domain of VP4 capsid protein mediates binding to $\alpha_2\beta_2$ integrins, and that this interaction is improved dependent on the cation-related conformation state of the receptor. Using a novel automated method, we identified that the binding interactions observed involved the formation of four uncorrelated non-covalent bonds based on the Williams-Evans Fit, whereas manual analysis only detected three.[101] Based on the observed interactions, we proposed that the bond formation being assessed was likely tied to the α_2 subunit of the integrin and explored the ability of a peptide based on the sequence of this domain to interfere with bond formation.[101] The predictive power granted *via* AFM allowing for the production of a novel therapeutic peptide that interferes with rotavirus binding and thus cellular entry.

Among the most illustrative examples of how AFM can be applied to aid in real-world biomedical applications is the role played in the rapid response to the COVID-19 global pandemic. The emergence and rapid spread of SARS-CoV-2 necessitated swift study to characterize even the most fundamental aspects of the virus' biology. Being differentiated from SARS-CoV and the original BatCoV RaTG13 by a number of alterations to the spike protein (S1), assessment of the binding and entry pathways accessible by the virus was a key focus at the beginning of the pandemic. Moreover, the wide diversity in symptomology and severity of disease suggested that underlying factors in communities may interfere with either the infection, cell-cell spread, or replication processes. Indicating that there may be important molecular determinants to be discovered, especially as the virus continues to mutate and the probability of a new SARS-CoV virus looms. In Yang *et al.* (2020),[35] we characterized the thermodynamics of the S1 receptor binding domain (RBD) interaction with the suspected key entry receptor angiotensin-converting enzyme 2 (ACE2). Wherein we have proven that the glycosylated RBD subunit of the spike trimer was required for the establishment of high affinity bonds with ACE2 (~120 nM) and as little difference was observed when using whole S1 glycoprotein trimer, this is likely the driving force behind this interaction.[35] Further, we have shown on both model surfaces and live cells that ACE2 derived peptides could interfere with the binding of the RBD fragment of S1.[35] Following this, we went on to examine the binding kinetics and behaviours of epidemiologically important variants of concern in Koehler *et al.* (2021).[102] Finding that while multivalent interactions with ACE2 were conserved in most

strains, the affinity of this interaction was improved in at least two examples, the Kappa and Gamma strains, with significantly

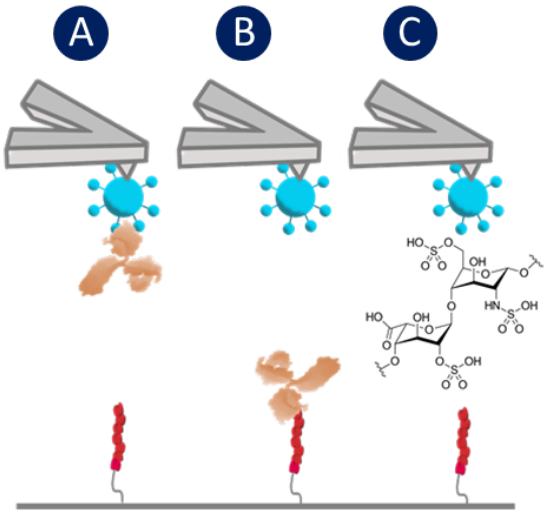

Figure 12: Examples of agents that can be screened for interfering with bond formation for therapeutic screening. **(a)** a neutralizing antibody, **(b)** a blocking antibody, **(c)** the injection of an inhibitory small molecule *e.g.:* heparin.

improved K_D values being retrieved from AFM experiments.[102] When combined with simulation data, interesting changes in energetics arising from specific mutations in the S1 RBD were found to be stabilized through Van der Waals forces yielding more intermolecular bonds and reinforcing the interface, in addition to long range Coulomb interactions in the Kappa variant.[102] Indicating that the key improvements in infectivity were tied more-so to the architecture of bond formation rather than the improvement of the high affinity interaction directly.[102]

To further expand on this, we reported that the bond between the SARS-CoV-2 S1 protein is differentially disrupted by neutralizing antibodies across the epidemiologically important strains for one example, showing that antibody therapeutics and those generated by natural immune processes vary in efficacy across these variants, and like those currently emerging, such as the recent Omicron derivative.

As highlighted in our studies of SARS-CoV-2,[35,102] rotavirus,[101] and herpesvirus,[103] the AFM techniques utilized can be used to rapidly screen for potential drug candidates that interfere with the formation of supramolecular bonds. Common examples being neutralizing antibodies, derivatives, nanobodies, and peptides, although small molecules, such as inhibitors can also be assessed in this manner (**Figure 12**). Being able to decipher the exact molecular mechanisms behind binding interactions allows for improved rational design, as exemplified in Yang *et al*. (2021),[101] wherein the AFM data was used to directly inform the production of a peptide sequence that blocked the interaction between rotavirus and integrins. The ability to rapidly screen potential therapeutics at a single molecule level and identify their ability to disrupt or interfere with the formation of the supramolecular bonds required for binding and entry of viruses is pertinent to developing efficacious therapies and presents an enormous opportunity to expand AFM into a more mainstream component of the pre-clinical pipeline.

Conclusions & Outlook

The power of AFM to interrogate the molecular interactions and bond formation in biomedical applications has improved rapidly and is near unparalleled. Being able to understand the chemical interactions that underly important physiological functions is a non-trivial matter. The ability to understand pathophysiology and treatment efficacy at a molecular level allows for improved rational design of novel therapeutics, application of existing treatments, and preventatives. We can now explore interactions in real-time at a nanoscale level and provide in-depth data regarding important interactions such as viral binding and entry, the surface chemistry of cells, and screen the ability of novel therapeutics to interfere with bond establishment.

As the ability to explore biological processes in tissue-like conditions and over longer time periods continues to improve, our ability to use AFM to shed light upon important molecular processes and interactions will also increase. The development of AFM compatible organoids, analysis of tissues ex vivo, and novel models hold the potential to improve our understanding of how disease states progress, therapeutics interact with targets, and pathogens interact under such circumstances. Given the power of AFM to assess binding phenomena quantitatively, this is of great potential importance to the development of targeted or personalised medicines, such as antibody-drug conjugates, nanobodies, and nanomedicines. As the capability of AFM continues to progress, it is highly likely this powerful technique will become a staple of the pre-clinical pipeline, and for understanding pathophysiology and therapy more broadly.

Conflicts of interest

There are no conflicts to declare.

Acknowledgements

This work was supported by the Université catholique de Louvain. The project received funding from the European Research Council under the European Union's Horizon 2020 research and innovation program (grant agreement no. 758224) and from the FNRS-Welbio (Grant # CR-2019S-01). M.K. and D. A. are postdoctoral researcher and Research Associate at the FNRS, respectively.

References

1 G. Binnig, C. F. Quate and C. Gerber, *Phys. Rev. Lett.*, 1986, **56**, 930–933.

2 N. Pavlicek and L. Gross, *Nat. Rev. Chem.*, 2017, **1**, 5.

3 D. J. Müller, A. C. Dumitru, C. Lo Giudice, H. E. Gaub, P. Hinterdorfer, G. Hummer, J. J. De Yoreo, Y. F. Dufrêne and

D. Alsteens, *Chem. Rev.*, 2021, **121**, 11701–11725.
4 D. Alsteens, H. E. Gaub, R. Newton, M. Pfreundschuh, C. Gerber and D. J. Müller, *Nat. Rev. Mater.*, , DOI:10.1038/natrevmats.2017.8.
5 A. Viljoen, M. Mathelié-Guinlet, A. Ray, N. Strohmeyer, Y. J. Oh, P. Hinterdorfer, D. J. Müller, D. Alsteens and Y. F. Dufrêne, *Nat. Rev. Methods Prim.*, 2021, **1**, 63.
6 C. D. Frisbie, L. F. Rozsnyai, A. Noy, M. S. Wrighton and C. M. Lieber, *Science*, 1994, **265**, 2071–2074.
7 M. Ludwig, W. Dettmann and H. E. Gaub, *Biophys. J.*, 1997, **72**, 445–448.
8 G. U. Lee, D. A. Kidwell and R. J. Colton, *Langmuir*, 1994, **10**, 354–357.
9 F. Ernst-Ludwig, M. V. T. and G. H. E., *Science*, 1994, **264**, 415–417.
10 P. Hinterdorfer, W. Baumgartner, H. J. Gruber, K. Schilcher and H. Schindler, *Proc. Natl. Acad. Sci. U. S. A.*, 1996, **93**, 3477–3481.
11 L. Wildling, B. Unterauer, R. Zhu, A. Rupprecht, T. Haselgrübler, C. Rankl, A. Ebner, D. Vater, P. Pollheimer, E. E. Pohl, P. Hinterdorfer and H. J. Gruber, *Bioconjug. Chem.*, 2011, **22**, 1239–1248.
12 C. Bustamante, J. F. Marko, E. D. Siggia and S. Smith, *Science*, 1994, **265**, 1599–1600.
13 G. U. Lee, L. A. Chrisey and R. J. Colton, *Science*, 1994, **266**, 771–773.
14 M. Rief, F. Oesterhelt, B. Heymann and H. E. Gaub, *Science (80-.).*, 1997, **275**, 1295–1297.
15 M. Grandbois, W. Dettmann, M. Benoit and H. E. Gaub, *J. Histochem. Cytochem.*, 2000, **48**, 719–724.
16 P. P. Lehenkari, G. T. Charras, A. Nykänen and M. A. Horton, *Ultramicroscopy*, 2000, **82**, 289–295.
17 V. Dupres, F. D. Menozzi, C. Locht, B. H. Clare, N. L. Abbott, S. Cuenot, C. Bompard, D. Raze and Y. F. Dufrêne, *Nat. Methods*, 2005, **2**, 515–520.
18 M. Benoit, D. Gabriel, G. Gerisch and H. E. Gaub, *Nat. Cell Biol.*, 2000, **2**, 313–317.
19 D. Alsteens, A. Beaussart, S. Derclaye, S. El-Kirat-Chatel, H. R. Park, P. N. Lipke and Y. F. Dufrêne, *Anal. Methods*, 2013, **5**, 3657–3662.
20 C. M. Stroh, A. Ebner, M. Geretschläger, G. Freudenthaler, F. Kienberger, A. S. M. Kamruzzahan, S. J. Smith-Gill, H. J. Gruber and P. Hinterdorfer, *Biophys. J.*, 2004, **87**, 1981–1990.
21 C. Stroh, H. Wang, R. Bash, B. Ashcroft, J. Nelson, H. Gruber, D. Lohr, S. M. Lindsay and P. Hinterdorfer, *Proc. Natl. Acad. Sci. U. S. A.*, 2004, **101**, 12503–12507.
22 M. Dong and O. Sahin, *Nat. Commun.*, , DOI:10.1038/ncomms1246.
23 Y. F. Dufrêne, T. Ando, R. Garcia, D. Alsteens, D. Martinez-Martin, A. Engel, C. Gerber and D. J. Müller, *Nat. Nanotechnol.*, 2017, **12**, 295–307.
24 D. Alsteens, R. Newton, R. Schubert, D. Martinez-Martin, M. Delguste, B. Roska and D. J. Müller, *Nat. Nanotechnol.*, 2017, **12**, 177–183.
25 M. Koehler, C. Lo Giudice, P. Vogl, A. Ebner, P. Hinterdorfer, H. J. Gruber and D. Alsteens, *Nano Lett.*, 2020, **20**, 4038–4042.
26 P. Saha, T. Duanis-Assaf and M. Reches, *Adv. Mater. Interfaces*, 2020, **7**, 1–14.
27 M. Targosz-Korecka, M. Jaglarz, K. E. Malek-Zietek, A. Gregorius, A. Zakrzewska, B. Sitek, Z. Rajfur, S. Chlopicki and M. Szymonski, *Sci. Rep.*, 2017, **7**, 15951.
28 A. Beaussart, S. El-Kirat-Chatel, P. Herman, D. Alsteens, J. Mahillon, P. Hols and Y. F. Dufrêne, *Biophys. J.*, 2013, **104**, 1886–1892.
29 A. Ishiwata, Y. J. Lee and Y. Ito, *Org. Biomol. Chem.*, 2010, **8**, 3596–3608.
30 D. Takamatsu, Y. Yamakoshi and K. Fukui, *J. Phys. Chem. B*, 2006, **110**, 1968–1970.
31 G. Chen, X. Ning, B. Park, G.-J. Boons and B. Xu, *Langmuir*, 2009, **25**, 2860–2864.
32 R. Kumar, S. N. Ramakrishna, V. V Naik, Z. Chu, M. E. Drew, N. D. Spencer and Y. Yamakoshi, *Nanoscale*, 2015, **7**, 6599–6606.
33 G. A. Lemieux and C. R. Bertozzi, *Trends Biotechnol.*, 1998, **16**, 506–513.
34 L. Schmitt, M. Ludwig, H. E. Gaub and R. Tampé, *Biophys. J.*, 2000, **78**, 3275–3285.
35 J. Yang, S. J. L. Petitjean, M. Koehler, Q. Zhang, A. C. Dumitru, W. Chen, S. Derclaye, S. P. Vincent, P. Soumillion and D. Alsteens, *Nat. Commun.*, 2020, **11**, 4541.
36 Z. Lv, R. Roychaudhuri, M. M. Condron, D. B. Teplow and Y. L. Lyubchenko, *Sci. Rep.*, 2013, **3**, 2880.
37 R. Newton, M. Delguste, M. Koehler, A. C. Dumitru, P. R. Laskowski, D. J. Müller and D. Alsteens, *Nat. Protoc.*, 2017, **12**, 2275–2292.
38 M. Koehler, P. Aravamudhan, C. Guzman-Cardozo, A. C. Dumitru, J. Yang, S. Gargiulo, P. Soumillion, T. S. Dermody and D. Alsteens, *Nat. Commun.*, 2019, **10**, 1–14.
39 L. Arnal, G. Longo, P. Stupar, M. F. Castez, N. Cattelan, R. C. Salvarezza, O. M. Yantorno, S. Kasas and M. E. Vela, *Nanoscale*, 2015, **7**, 17563–17572.
40 R. Louise Meyer, X. Zhou, L. Tang, A. Arpanaei, P. Kingshott and F. Besenbacher, *Ultramicroscopy*, 2010, **110**, 1349–1357.
41 G. Zeng, T. Müller and R. L. Meyer, *Langmuir*, 2014, **30**, 4019–4025.
42 F. Kienberger, A. Ebner, H. J. Gruber and P. Hinterdorfer, *Acc. Chem. Res.*, 2006, **39**, 29–36.
43 J. A. Craig, E. L. Rexeisen, A. Mardilovich, K. Shroff and E. Kokkoli, *Langmuir*, 2008, **24**, 10282–10292.
44 H. Lei, Q. Ma, W. Li, J. Wen, H. Ma, M. Qin, W. Wang and Y. Cao, *Nat. Commun.*, 2021, **12**, 5082.
45 M. E. Drew, A. R. Konicek, P. Jaroenapibal, R. W. Carpick and Y. Yamakoshi, *J. Mater. Chem.*, 2012, **22**, 12682–12688.
46 G. Pyrgiotakis, C. O. Blattmann and P. Demokritou, *ACS Sustain. Chem. Eng.*, 2014, **2**, 1681–1690.
47 Q. K. Ong and I. Sokolov, *J. Colloid Interface Sci.*, 2007, **310**, 385–390.
48 W. A. Ducker, T. J. Senden and R. M. Pashley, *Nature*, 1991, **353**, 239–241.
49 T. Harayama and H. Riezman, *Nat. Rev. Mol. Cell Biol.*,

2018, **19**, 281–296.
50 R. Butti, S. Das, V. P. Gunasekaran, A. S. Yadav, D. Kumar and G. C. Kundu, *Mol. Cancer*, 2018, **17**, 34.
51 G. Yan, M. E. M. Saeed, S. Foersch, J. Schneider, W. Roth and T. Efferth, *Oncotarget*, 2019, **10**, 1918–1931.
52 L. M. Butler, Y. Perone, J. Dehairs, L. E. Lupien, V. de Laat, A. Talebi, M. Loda, W. B. Kinlaw and J. V Swinnen, *Adv. Drug Deliv. Rev.*, 2020, **159**, 245–293.
53 A. C. Dumitru, A. Stommen, M. Koehler, A.-S. Cloos, J. Yang, A. Leclercqz, D. Tyteca and D. Alsteens, *Nano Lett.*, 2021, **21**, 4950–4958.
54 Z. Erami, D. Herrmann, S. C. Warren, M. Nobis, E. J. McGhee, M. C. Lucas, W. Leung, N. Reischmann, A. Mrowinska, J. P. Schwarz, S. Kadir, J. R. W. Conway, C. Vennin, S. A. Karim, A. D. Campbell, D. Gallego-Ortega, A. Magenau, K. J. Murphy, R. A. Ridgway, A. M. Law, S. N. Walters, S. T. Grey, D. R. Croucher, L. Zhang, H. Herzog, E. C. Hardeman, P. W. Gunning, C. J. Ormandy, T. R. J. Evans, D. Strathdee, O. J. Sansom, J. P. Morton, K. I. Anderson and P. Timpson, *Cell Rep.*, 2016, **14**, 152–167.
55 K. Mukund and S. Subramaniam, *WIREs Syst. Biol. Med.*, 2020, **12**, e1462.
56 J. J. Liu, A. Hezghia, S. R. Shaikh, J. F. Cenido, R. E. Stark, J. J. Mann and M. E. Sublette, *Neuropsychopharmacol. Rep*, 2018, **43**, 2165–2179.
57 A. C. Dumitru, D. Mohammed, M. Maja, J. Yang, S. Verstraeten, A. del Campo, M.-P. Mingeot-Leclercq, D. Tyteca and D. Alsteens, *Adv. Sci.*, 2020, **7**, 2002643.
58 D. K. Verma, D. Gupta and S. K. Lal, *Viruses* , 2018, **10**, 650-661.
59 J. D. Greenlee, T. Subramanian, K. Liu and M. R. King, *Cancer Res.*, 2021, **81**, 5 LP – 17.
60 E. Dague, D. Alsteens, J.P. Latgé, C. Verbelen, D. Raze, A. R. Baulard and Y. F. Dufrêne, *Nano Lett.*, 2007, **7**, 3026–3030.
61 D. Alsteens, E. Dague, P. G. Rouxhet, A. R. Baulard and Y. F. Dufrêne, *Langmuir*, 2007, **23**, 11977–11979.
62 Y. F. Dufrêne, *Trends Microbiol.*, 2015, **23**, 376–382.
63 A. C. Dumitru, M. A. Poncin, L. Conrard, Y. F. Dufrêne, D. Tyteca and D. Alsteens, *Nanoscale Horiz*, 2018, **3**, 293–304.
64 K. G. Rothberg, Y. S. Ying, B. A. Kamen and R. G. Anderson, *J. Cell Biol.*, 1990, **111**, 2931–2938.
65 P. J. A., Y. K. E. and B. P. A., *Science*, 1996, **274**, 255–259.
66 X. Xiao, J.-J. Tang, C. Peng, Y. Wang, L. Fu, Z.-P. Qiu, Y. Xiong, L.-F. Yang, H.-W. Cui, X.-L. He, L. Yin, W. Qi, C. C. L. Wong, Y. Zhao, B.-L. Li, W.-W. Qiu and B.-L. Song, *Mol. Cell*, 2017, **66**, 154-162.e10.
67 R. Sheng, H. Kim, H. Lee, Y. Xin, Y. Chen, W. Tian, Y. Cui, J.-C. Choi, J. Doh, J.-K. Han and W. Cho, *Nat. Commun.*, 2014, **5**, 4393.
68 A. C. Dumitru, L. Conrard, C. Lo Giudice, P. Henriet, M. Veiga-da-Cunha, S. Derclaye, D. Tyteca and D. Alsteens, *Chem. Commun.*, 2018, **54**, 6903–6906.
69 B. B. Johnson, M. Breña, J. Anguita and A. P. Heuck, *Sci. Rep.*, 2017, **7**, 13793.
70 A. C. Dumitru, R. N. V. K. Deepak, H. Liu, M. Koehler, C. Zhang, H. Fan and D. Alsteens, *Commun. Biol.*, 2020, **3**, 786.
71 G. Servant, O. D. Weiner, E. R. Neptune, J. W. Sedat and H. R. Bourne, *Mol. Biol. Cell*, 1999, **10**, 1163–1178.
72 F. H. Brennan, R. Gordon, H. W. Lao, P. J. Biggins, S. M. Taylor, R. J. M. Franklin, T. M. Woodruff and M. J. Ruitenberg, *J. Neurosci.*, 2015, **35**, 6517 LP – 6531.
73 P. A. Ward, *J. Mol. Med.*, 2009, **87**, 375–378.
74 T. M. Woodruff, K. S. Nandakumar and F. Tedesco, *Mol. Immunol.*, 2011, **48**, 1631–1642.
75 H. Hawlisch, M. Wills-Karp, C. L. Karp and J. Köhl, *Mol. Immunol.*, 2004, **41**, 123–131.
76 E. Panayiotou, E. Fella, S. Andreou, R. Papacharalambous, P. Gerasimou, P. Costeas, S. Angeli, I. Kousiappa, S. Papacostas and T. Kyriakides, *PLoS One*, 2019, **14**, e0225417.
77 Z. Wang, W. Yu, Y. Qiang, F. Ma, P. Ding and Y. Wang, *BMC Cancer*, 2021, **21**, 1136.
78 A. Stylianou, M. Lekka and T. Stylianopoulos, *Nanoscale*, 2018, **10**, 20930–20945.
79 J. Solon, I. Levental, K. Sengupta, P. C. Georges and P. A. Janmey, *Biophys. J.*, 2007, **93**, 4453–4461.
80 J. Rheinlaender, A. Dimitracopoulos, B. Wallmeyer, N. M. Kronenberg, K. J. Chalut, M. C. Gather, T. Betz, G. Charras and K. Franze, *Nat. Mater.*, 2020, **19**, 1019–1025.
81 I. Andreu, B. Falcones, S. Hurst, N. Chahare, X. Quiroga, A.-L. Le Roux, Z. Kechagia, A. E. M. Beedle, A. Elosegui-Artola, X. Trepat, R. Farré, T. Betz, I. Almendros and P. Roca-Cusachs, *Nat. Commun.*, 2021, **12**, 4229.
82 A. Rigato, A. Miyagi, S. Scheuring and F. Rico, *Nat. Phys.*, 2017, **13**, 771–775.
83 M. LeClaire, J. A. Wohlschlegel, H. Chang, M. Wadehra, W. Yu, J. Rao, D. Elashoff, J. K. Gimzewski and S. Sharma, *ACS Appl. Nano Mater.*, 2021, **4**, 9876–9885.
84 D. Mohammed, M. Koehler, A. C. Dumitru, P. Aravamudhan, D. M. Sutherland, T. S. Dermody and D. Alsteens, *Nano Lett.*, 2021, **21**, 9720–9728.
85 A. F. Guedes, F. A. Carvalho, I. Malho, N. Lousada, L. Sargento and N. C. Santos, *Nat. Nanotechnol.*, 2016, **11**, 687–692.
86 C. L. Essmann, D. Martinez-Martinez, R. Pryor, K.-Y. Leung, K. B. Krishnan, P. P. Lui, N. D. E. Greene, A. E. X. Brown, V. M. Pawar, M. A. Srinivasan and F. Cabreiro, *Nat. Commun.*, 2020, **11**, 1043.
87 M. Li, L. Liu, N. Xi and Y. Wang, *Acta Pharmacol. Sin.*, 2015, **36**, 769–782.
88 F. Zuttion, A. Colom, S. Matile, D. Farago, F. Pompeo, J. Kokavecz, A. Galinier, J. Sturgis and I. Casuso, *Nat. Commun.*, 2020, **11**, 6312.
89 M. Koehler, S. J. L. Petitjean, J. Yang, P. Aravamudhan, X. Somoulay, C. Lo Giudice, M. A. Poncin, A. C. Dumitru, T. S. Dermody and D. Alsteens, *Nat. Commun.*, 2021, **12**, 1–15.
90 M. Mathelié-Guinlet, F. Viela, G. Pietrocola, P. Speziale, D. Alsteens and Y. F. Dufrêne, *Nat. Commun.*, 2020, **11**, 5431.
91 L. Lecordier, S. Uzureau, G. Vanwalleghem, M. Deleu, J.-M. Crowet, P. Barry, B. Moran, P. Voorheis, A.-C. Dumitru, Y. Yamaryo-Botté, M. Dieu, P. Tebabi, B. Vanhollebeke, L. Lins, C. Y. Botté, D. Alsteens, Y. Dufrêne, D. Pérez-Morga, D. P. Nolan and E. Pays, *iScience*, 2020, **23**, 101476.
92 A. Viljoen, D. Alsteens and Y. Dufrêne, *Cells* , 2020, 9.

93 V. Prystopiuk, C. Feuillie, P. Herman-Bausier, F. Viela, D. Alsteens, G. Pietrocola, P. Speziale and Y. F. Dufrêne, *ACS Nano*, 2018, **12**, 3609–3622.

94 M. Koehler, M. Delguste, C. Sieben, L. Gillet and D. Alsteens, *Annu. Rev. Virol.*, 2020, **7**, 143–165.

95 S. P. Yamamoto, D. Motooka, K. Egawa, A. Kaida, Y. Hirai, H. Kubo, K. Motomura, S. Nakamura and N. Iritani, *Sci. Rep.*, 2020, **10**, 1–7.

96 J. E. Strong, M. C. Coffey, D. Tang, P. Sabinin and P. W. K. Lee, *EMBO J.*, 1998, **17**, 3351–3362.

97 K. L. Norman, K. Hirasawa, A.-D. Yang, M. A. Shields and P. W. K. Lee, *Proc. Natl. Acad. Sci. U. S. A.*, 2004, **101**, 11099 LP – 11104.

98 J. R. Diller, S. R. Halloran, M. Koehler, R. dos Santos Natividade, D. Alsteens, T. Stehle, T. S. Dermody and K. M. Ogden, *J. Virol.*, 2020, **94**, e01163-20.

99 J. S. Carew, C. M. Espitia, W. Zhao, K. R. Kelly, M. Coffey, J. W. Freeman and S. T. Nawrocki, *Cell Death Dis.*, 2013, **4**, e728–e728.

100 M. Delguste, C. Zeippen, B. Machiels, J. Mast, L. Gillet and D. Alsteens, *Sci. Adv.*, 2018, **4**, eaat1273.

101 J. Yang, J. Park, M. Koehler, J. Simpson, D. Luque, J. M. Rodríguez and D. Alsteens, *Adv. NanoBiomed Res.*, 2021, **1**, https://doi.org/10.1002/anbr.202100077

102 M. Koehler, A. Ray, R. A. Moreira, B. Juniku, A. B. Poma and D. Alsteens, *Nat. Commun.*, 2021, **12**, 6977.

103 M. Delguste, G. Le Brun, F. Cotin, B. Machiels, L. Gillet and D. Alsteens, *Nano Lett.*, 2021, **21**, 847–853.